

Comparative Study on the Mg Doped Hydroxyapatite through Sol-gel and Hydrothermal Techniques

Abinaya R, Subha B, Adhilakshmi A and Ravichandran K*
Department of Analytical Chemistry, School of Chemical Sciences,
University of Madras, Chennai, India.

Corresponding Author's Email: raavees@gmail.com

Abstract - The aim of this study was to compare the sol-gel and hydrothermally synthesized pure and magnesium doped hydroxyapatite. Calcium nitrate tetrahydrate, magnesium nitrate hexahydrate and ammonium dihydrogen phosphate were used as a precursor for Ca, Mg and P in both methods. The synthesized powder was sintered at 800°C. The samples were characterized by Fourier Transform Infrared Spectroscopy for functional group analysis, X-Ray Diffraction for crystallinity and phase purity analysis, Scanning Electron Microscopy coupled with Energy dispersive X-Ray for morphological analysis and (Ca+Mg)/P ratio. Simulated Body Fluid is prepared by using chlorides, carbonates, oxides and sulphates of alkali metals at 37°C. The bioresorbability of sol-gel and hydrothermally synthesized materials has been examined in vitro by immersing in simulated body fluid and measuring the variation of pH. The results obtained shows that Hydroxyapatite synthesized by both methods are bioresorbable. However, the hydrothermally synthesized pure and Magnesium doped hydroxyapatite revealed a higher resorbability. The FTIR shows the influence of Mg and XRD results confirmed presence of Mg in the lattice structure of HAP. The crystal size is found to be in the range of 10nm-40nm. Scanning Electron Micrographs confirms the influence of Mg on the morphology and particle size.

Keywords: Hydroxyapatite, dopant, Sol-gel, Hydrothermal

I. INTRODUCTION

Bone tissue has a high regenerative capacity for self repair on damage. This self repairing process often fails when the bone defects are too large or the natural healing capacity is insufficient. The recent strategies for repairing and reconstructing these large bone defects use bone grafting materials such as autografts, allografts and xenografts. However, limitations in those approaches viz., the limited availability, possibility of disease transmission and poor biocompatibility have all increased the necessity of artificial synthetic bone implants incorporating ceramics like calcium phosphate materials on its surface^[1]. The biomineral phase, which is one or more type of calcium phosphates, comprises 65-70% of bone, water accounts for 5-8% and the organic phase, like collagen, accounts for the remainder. The collagen, which gives the bone its elastic resistance, acts as a matrix for the deposition and growth of minerals. Among the calcium phosphate salts, hydroxyapatite is the thermodynamically most stable crystalline phase of calcium phosphate in body fluid^[2].

Hydroxyapatite [HAP] constitutes the main mineral components of bone and teeth. Stoichiometric HAP has the composition $\text{Ca}_{10}(\text{PO}_4)_3(\text{OH})_2$ with Ca/P ratio of 1.67^[3]. Thus it is commonly used as a filler to replace amputated bone or coating to promote bone ingrowth over the prosthetic implants. Recently hip replacement and dental implants are coated with HAP. It has been reported that this may promote osseointegration. Porous HAP implants are used for localized local drug delivery in the affected areas of bones^[4]. Due to its growing importance and applications numerous techniques have been reported for the synthesis of HAP^[5]. Important techniques being used are solid state reaction^[6], co-precipitation^[7], emulsion^[8], microwave synthesis^[9, 10], etc., and produce HAP in different forms. Most of these methods have significant limitations such as low mechanical strength in the coating, high temperature requirement, inhomogeneous microstructure and loss of crystallinity. In order to avoid such limitations, the hydrothermal method^[11, 12] and sol-gel route^[7, 12-17] has been developed.

Many substitutions can be introduced to HAP structure to improve its biocompatibility and bioactivity. Especially, the presence of strontium (Sr) enhances osteoblast activity and differentiation^[18, 19], silicon (Si) enhances the formation of a poorly crystalline surface apatite layer of HAP after immersing in simulated body fluid (SBF)^[20, 21], Zinc (Zn) incorporated into HAP may promote bone formation around the material and also to prevent or minimize the initial bacterial adhesion^[22, 23], Magnesium (Mg) is known to be an important trace element, particularly during the early stages of osteogenesis where it stimulates osteoblast proliferation and its depletion causes bone fragility and bone loss. Furthermore, relationship has been suggested between the Mg content in enamel and the development of dental caries. Giving the biological relevance of Mg, many researchers have worked on the preparation of HAP and calcium phosphate implant materials containing low

level of Mg, which has been showed to improve biological role of Mg^[24, 25]. The presence of Mg in HAP inhibits crystallization, reduces crystal size and decreases the proliferation and activity of osteoblast like cells, while its deficiency affects all stages of skeletal metabolism, causing cessation of bone growth, decrease of osteoblastic and osteoclastic activities and bone fragility^[1]. In short, it is considered as one of the most important trace element in HAP.

Hence, the primary objective of this study was the incorporation of Mg ion in HAP by sol-gel and hydrothermal method and using calcium nitrate, magnesium nitrate and ammonium dihydrogen phosphate reagents as a precursors and to explore the impact of the Mg concentration on HAP crystal structure and as well as to compare the chemical and biological properties of the pure and Mg doped HAP synthesized through these methods.

II. EXPERIMENTAL METHODS

A. Reagents

Reagent grade chemicals such as calcium nitrate tetrahydrate $\text{Ca}(\text{NO}_3)_2 \cdot 4\text{H}_2\text{O}$, magnesium nitrate hexahydrate $\text{Mg}(\text{NO}_3)_2 \cdot 6\text{H}_2\text{O}$, ammonium dihydrogen phosphate $\text{NH}_4\text{H}_2\text{PO}_4$, liquid ammonia and absolute ethanol (99%) obtained from Merck and used as starting chemical precursors. All solutions were prepared either in pure ethanol or in double distilled water.

B. Sol-Gel method

To synthesis magnesium doped HAP through sol-gel processing, target amount of $\text{Mg}(\text{NO}_3)_2 \cdot 6\text{H}_2\text{O}$ from 0, 0.1, 0.3 and 0.5mole ratios were incorporated into the sol of $\text{Ca}(\text{NO}_3)_2 \cdot 4\text{H}_2\text{O}$. The mixture of Ca and Mg was stirred for 1 hour. The sol was added drop wise into the $\text{NH}_4\text{H}_2\text{PO}_4$ with vigorous stirring at a temperature of 85°C. The pH of the sol was maintained by using liquid NH_3 . As a result of the above process, the so-prepared solutions were transformed into white gel after a period of 4 hours and it is further aged at room temperature for 24 hours. The aged gel was dried at 100°C and sintered at 800°C for 2 hours.

C. Hydrothermal method

In hydrothermal technique, $\text{Ca}(\text{NO}_3)_2 \cdot 4\text{H}_2\text{O}$ and $\text{Mg}(\text{NO}_3)_2 \cdot 6\text{H}_2\text{O}$ were prepared in double distilled water and the pH was adjusted to 11 with liquid NH_3 , in which molar ratio of the Ca to Mg were maintained at 0, 0.1, 0.3, 0.5 M respectively. The mixture of Ca and Mg ions was stirred for 1 hour on room temperature. The above mixture was added drop wise to the solution of $\text{NH}_4\text{H}_2\text{PO}_4$ and brought to pH 11 using liquid NH_3 with vigorous stirring for 2 hours to produce white precipitate. The precipitate was then kept in a Teflon coated autoclave at 150°C for 5 hours. The precipitate was filtered, washed repeatedly with double distilled water and dried in air oven at 100°C. The resulting powder was finally sintered at 800°C for 2 hours.

D. Characterization

Appropriate techniques were used to characterize thus synthesized powders. The crystalline phases present were identified by X-ray diffraction (GE-X-Ray Diffraction-XRD 3003 TT) using Cu K radiation at 50 kV voltage and 100 mA current, the agglomeration, morphology and particle sizes and the Ca, Mg and P content of the samples were determined with Scanning electron Microscope (SEM), the instrument Philips 501 scanning electron microscope (SEM) equipped with energy dispersive X-ray microanalysis (EDX). The samples were coated with thin layer of gold using Edwards sputter coater S150B instrument. Fourier Transform Infrared spectroscopy (Agilent Cary-630 FTIR spectrometer) was employed to identify the functional groups. The in-vitro bioresorbability tests of the samples were conducted by immersing samples in simulated body fluid (SBF) at pH 7.4. The SBF solution was prepared by using kokubos protocol^[26]. Each sample (1mg/ml) was immersed in 50ml of SBF at 37°C for 14 days. The pH of the SBF solution was measured (ELICO LI 120 pH meter) every day during the soaking periods of 0 to 14 days.

III. RESULT AND DISCUSSION

A. Infrared spectroscopy

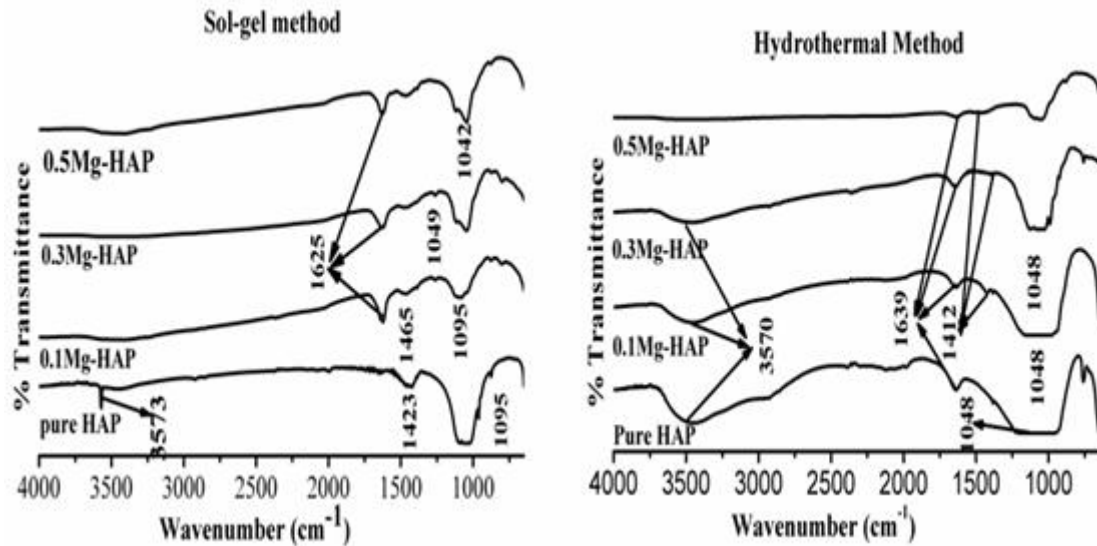


Figure 1: FTIR spectra of pure and Mg doped HAP

Figure 1 are represents the FTIR spectra sol gel and hydrothermally produced pure and Mg doped HAP samples. All these samples displayed the vibrational modes of PO_4^{3-} and OH group characteristics of HAP. There is a broad envelope between 3600cm^{-1} to 3200cm^{-1} which represents to OH stretching vibrations of water and HAP. The peak around 1636cm^{-1} is assigned to bending mode of water. The absorption band around 1412 , 1423cm^{-1} is attributed to the presence of CO_3^{2-} in the samples. The intense broad peak between 900cm^{-1} and 1100cm^{-1} is assigned to PO_4^{3-} . Kuriakose et al^[5] reported dissolving of atmospheric CO_2 to CO_3^{2-} based on the peak of 1456cm^{-1} and 873cm^{-1} as the crystallization was carried out in pH 11. The peak observed around 3570cm^{-1} is the characteristic peak corresponding to stoichiometric HAP. Previous reports suggested, the Mg-HAP shows decreased intensity of OH vibration modes at those bands with respect to HAP samples. It can be explained by the increased lattice due to HPO_4^{2-} substitution^[1]. As seen in figure 1, it was evident that the intensity of those peak decreases with increasing the Mg content.

B. X-Ray Diffraction Analysis

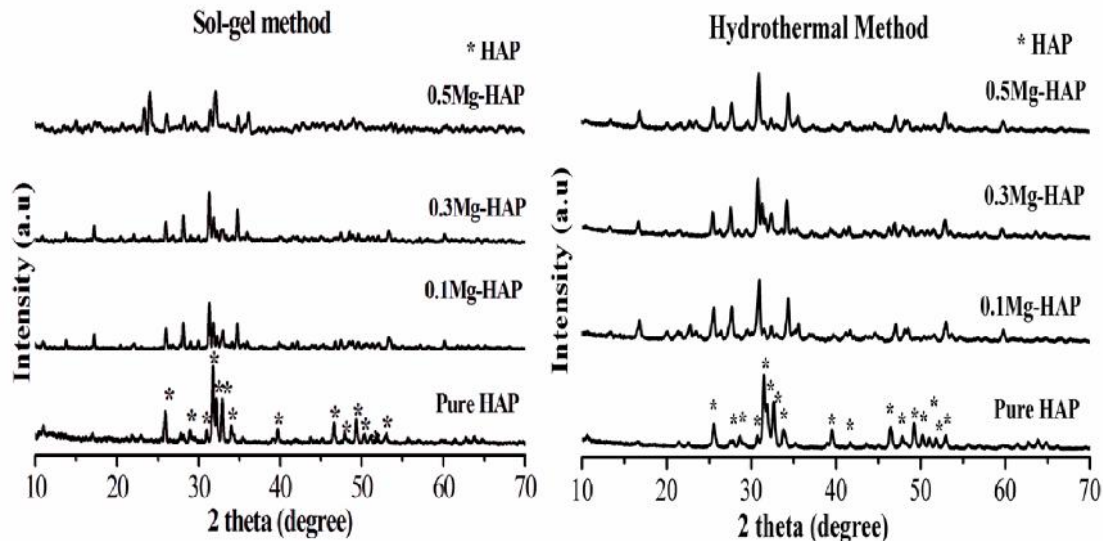


Figure 2: XRD pattern of pure and Mg doped HAP

XRD data of pure and Mg doped HAP of sol-gel and hydrothermal techniques were recorded in the 2 θ range of 10° to 70°. The resulting XRD patterns were shown in Figure 2. The HAP diffraction peaks for all samples according to standard JCPDS cards, indicating that the Mg ion entered into the crystal lattice HAP and occupied Ca²⁺ sites. In XRD pattern indicates that all the synthesized samples are composed of pure apatite phase (no secondary phase) except sol-gel synthesized 0.5M Mg doped HAP. The sharp peaks confirms they were well crystallized. The relative intensity of major diffraction peaks decreased and some peaks disappeared with increasing Mg content. HPO₄²⁻ peak was observed in 0.5M Mg doped HAP in sol-gel technique, another significant observation was the conversion of from hexagonal to rhombohedral phase according to the JCPDS card no 00-6190. The crystal size of the all the samples were calculated by using Debye Scherrer relationship based on line broadening in the XRD pattern.

$$d = K\lambda/\beta\cos\theta$$

The average crystal size of sol-gel synthesized pure HAP was 25nm, where as the average size of the crystals obtained from 0.1, 0.3M Mg doped HAP was 34nm. The increase in particle size may be due to the destruction in HAP crystal structure. However, with 0.5M Mg doped HAP the crystal size was 16nm it may be due to the contraction in crystal structure. In hydrothermal method, the crystal size of pure HAP is 10nm, where as in 0.1, 0.3, and 0.5M Mg doped HAP the crystal size was 21nm, 19nm and 20nm. Compared both sol-gel and hydrothermal method, hydrothermally synthesized samples has smaller crystal size than the sol-gel synthesized samples.

C. SEM/EDX evolution

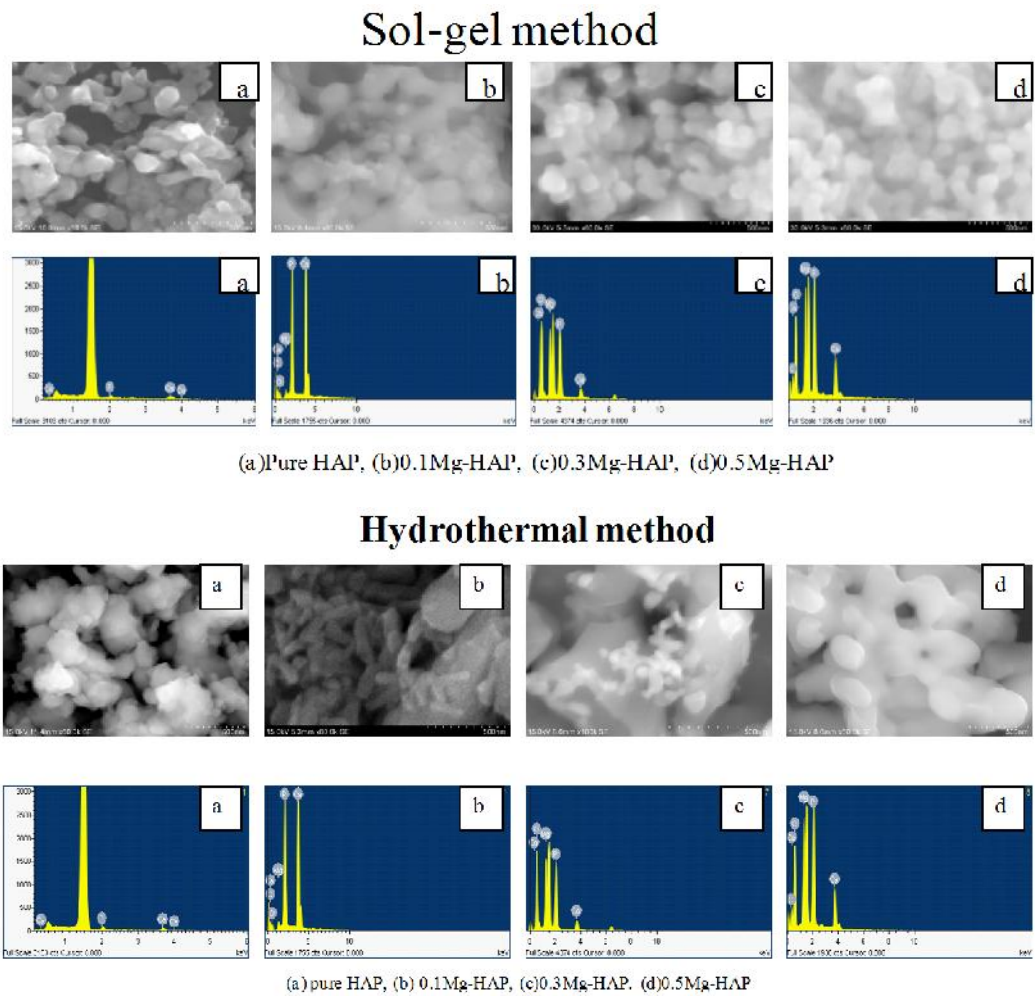


Figure 3: SEM images and EDX spectra of pure and Mg doped HAP

The morphological features and EDX patterns of the pure and Mg doped HAP obtained through sol-gel and hydrothermal method was illustrated in figure 3. The EDX results confirms the existence of the elements such as Ca, Mg, P and O besides it can be seen that the (Ca+Mg)/P ratio varies from 0.97 to 1.59, which indicates that the formed HAP is deficient in calcium content. The (Ca+Mg)/P ratio of the prepared samples depends on the pH value and dopants concentration. In sol-gel synthesized samples, the pure HAP consist of agglomerated HAP particles of uneven shape, whereas, in 0.1 and 0.3M Mg doped HAP revealed a sphere form with little agglomeration. In 0.5M Mg doped HAP produced uniformly arranged sphere shape.

In hydrothermally synthesized samples, the pure HAP revealed similar agglomeration of fine crystallites that cannot be seen individually in micrographs because of their small size. The 0.1 and 0.3M Mg doped HAP, produced rod like structure and 0.5M Mg doped HAP produced sphere shape. As dopant concentration increases, rod shape changes to the sphere one. The average particle sizes of both sol-gel and hydrothermally synthesized samples were around 10 to 100nm.

D. In-vitro Bioresorbability Analysis

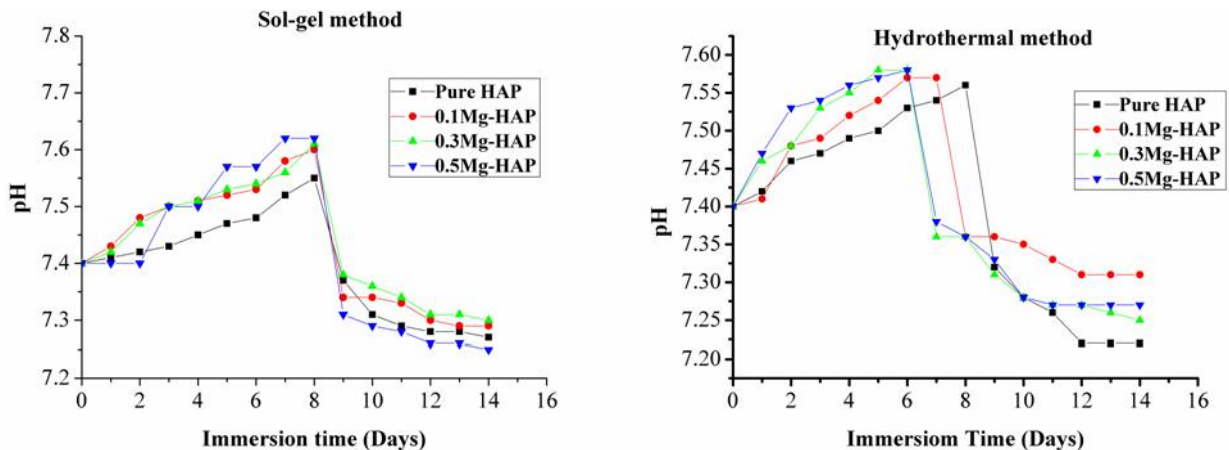


Figure 4: in vitro bioresorbability of pure and Mg doped HAP

Bioresorbability analysis of the pure and Mg doped HAP of sol-gel and hydrothermally synthesized was illustrated in figure 4. The test illustrates the dissolution of ions from the HAP (increase in pH) lattice and utilization of those ions (decrease in pH) for further apatite growth in SBF. Both solubility and resorbability processes are dependent on soaking time. Samples from both methods showed an initial pH increase with increase in immersion time and subsequent decrease. Initial pH increases is due to the release of Ca, Mg and PO_4^{3-} ions from the samples. The pH raise depends on solubility of the HAP and also with immersion time in SBF. From the figure 4, it is clear that there were notable evidence for solubility and resorbability of all the samples but dopant concentration and particle size influence the extent of both processes. The hydrothermally synthesized material was more soluble and resorbable.

IV. CONCLUSION

In this study, various concentration of Mg-doped HAP powders were synthesized by two different methods namely sol-gel and hydrothermal. The FTIR results indicated that the hydroxyl and phosphate peak intensity decreases with increasing Mg concentration. The XRD data showed the lattice parameters of HAP are influenced by Mg as a dopant. The Mg was well incorporated with the HAP lattice. The calculated crystal size through hydrothermal route having the lower crystal size compare to the sol-gel. Variations in morphology of HAP were observed with Mg content as well as with synthetic methodology. EDX analysis performed for determining the (Ca+Mg)/P ratio, HAP by the hydrothermal route produced nearer stoichiometric value then the sol-gel route. The bioresorbability of HAP can be altered by dopant concentration and particle size. Hence, the hydrothermal route was more bioactive than the sol-gel route. The obtained pure and Mg-doped HAP can be used for various biomedical applications.

ACKNOWLEDGMENT

The authors acknowledge the access to X-Ray Diffraction and electron microscopy facilities provided by the National Centre for Nano Science and Nano Technology (NCNSNT) and Nuclear Physics, University of Madras, Chennai, India.

REFERENCE

1. Salima Ziani, Samira Meski, and Hafit Khireddine, "Characterization of Magnesium-Doped Hydroxyapatite Prepared by Sol-Gel Process", International Journal of Applied Ceramic Technology, Vol. 11, No. 1, pp.83-91, 2014.
2. Mehdi Sadat-Shojai, Mohammad-Taghi Khorasani, Ehsan Dinpanah-Khoshdargi, Ahmad Jamshidi, "Synthesis methods for nanosized hydroxyapatite with diverse structures", Acta Biomaterialia, Vol. 9, pp. 7591–7621, 2013.
3. Matthew Bilton, Steven J. Milne, Andrew P. Brown, "Comparison of Hydrothermal and Sol-Gel Synthesis of Nano-Particulate Hydroxyapatite by Characterisation at the Bulk and Particle Level", Open Journal of Inorganic Non-metallic Materials, Vol. 2, pp.1-10, 2012.
4. Khairy Mohamed Tohamy Ereiba, A. G. Mostafa, G. A. Gamal, A. H. Said, "In vitro study of iron doped hydroxyapatite", Journal of Biophysical Chemistry Vol.4, pp.122-130, 2013.
5. T. Anee Kuriakose, S. Narayana Kalkuraa, M. Palanichamy, D. Arivuoli, Karsten Dierks, G. Bocelli, C. Betzel, "Synthesis of stoichiometric nano crystalline hydroxyapatite by ethanol-based sol-gel technique at low temperature", Journal of Crystal Growth Vol.263, pp.517–523, 2004.
6. R. Ramachandra Rao, H.N. Roopa, T.S. Kannan, "Solid state synthesis and thermal stability of HAP and HAP - beta-TCP composite ceramic powders", J. Mater. Sci. Mater. Med. Vol.8, pp.511, 1997
7. C. Guzmán Vázquez, C. Piña Barba, and N. Munguía, "Stoichiometric hydroxyapatite obtained by precipitation and sol gel processes", Revista Mexicana De Física, Vol.51, No.3, pp. 284–293, 2005.
8. Susmita Bose, Susanta Kumar Saha, "Synthesis and Characterization of Hydroxyapatite Nanopowders by Emulsion Technique", Chem. Mater Vol.15, pp.4464-4469, 2003.
9. A. Farzadi, M. Solati-Hashjin, F. Bakhshi, A. Aminian, "Synthesis and characterization of hydroxyapatite/beta-tricalciumphosphate nanocomposites using microwave irradiation", Ceramics International, Vol. 37, pp.65–71, 2011.
10. Walid Amer, Karima Abdelouahdi, Hugo Ronald Ramanarivo, Mohamed Zahouily, Aziz Fihri, Kamal Djessas, Khalid Zahouily, Rajender S. Varma and Abderrahim Solhy, "Microwave-assisted synthesis of mesoporous nano-hydroxyapatite using surfactant templates", CrystEngComm, Vol. 16, pp.543-549, 2014.
11. Edward Lester, Selina V. Y. Tang, Andrei Khlobystov, Vanessa Loczenski Rose, Lee Buttery and Clive J. Roberts, "Producing nanotubes of biocompatible hydroxyapatite by continuous hydrothermal synthesis", CrystEngComm, Vol.15, pp.3256-3260, 2013.
12. Matthew Bilton, Steven J. Milne, Andrew P. Brown, "Comparison of Hydrothermal and Sol-Gel Synthesis of Nano-Particulate Hydroxyapatite by Characterisation at the Bulk and Particle Level", Open Journal of Inorganic Non-metallic Materials, Vol.2, pp.1-10, 2012.
13. Khelendra Agrawal, Gurbhinder Singh, Devendra Puri, Satya Prakash, "Synthesis and Characterization of Hydroxyapatite Powder by Sol-Gel Method for Biomedical Application", Journal of Minerals & Materials Characterization & Engineering, Vol. 10, No.8, pp.727-734, 2011.
14. M.Bilton1, A.P. Brown, S. J. Milne, "Sol-gel synthesis and characterisation of nano-scale Hydroxyapatite", Journal of Physics: Conference Series 241, 012052, 2012.
15. Gréta Gergely, Ferenc Wéber, István Lukács, Levente Illés, Attila L. Tóth, Zsolt E. Horváth, Judit Mihály, Csaba Balázi, "Nano-hydroxyapatite preparation from biogenic raw materials", Cent. Eur. J. Chem. Vol.8, No.2, pp.375–381, 2010.
16. G. Suresh Kumar, E.K. Girija, A. Thamizhavel, Y. Yokogawa, S. Narayana Kalkura, "Synthesis and characterization of bioactive hydroxyapatite-calcite nanocomposite for biomedical applications", Journal of Colloid and Interface Science, Vol.349, pp.56–62, 2010.
17. A. Bigi, E. Boanini, and K. Rubini, "Hydroxyapatite gels and nanocrystals prepared through a sol-gel process", Journal of Solid State Chemistry, Vol.177, pp.3092–3098, 2004.
18. M.D. O'Donnell, Y. Fredholm, A. de Rouffignac, R.G. Hill, "Structural analysis of a series of strontium-substituted apatites", Acta Biomaterialia Vol.4, pp.1455–1464, 2008.
19. C. Capuccini, P. Torricelli, E. Boanini, M. Gazzano, R. Giardino, A. Bigi, "Interaction of Sr-doped hydroxyapatite nanocrystals with osteoclast and osteoblast-like cells", J. Biomed. Mater. Res. Vol.89A, pp.594–600, 2009.
20. E. S. Thian, J. Huang, S. M. Best, Z. H. Barber, W. Bonfield, "Novel Silicon-Doped Hydroxyapatite (Si-HA) for Biomedical Coatings: An In Vitro Study Using Acellular Simulated Body Fluid", J. Biomed. Mater. Res. Part B: Appl. Biomater. Vol.76B, pp.326–333, 2006.
21. Kentaro Nakata1, Takashi Kubo1, Chiya Numako, Takamasa Onoki and Atsushi Nakahira, "Synthesis and Characterization of Silicon-Doped Hydroxyapatite", Materials Transactions, Vol.50, No.5, pp. 1046-1049, 2009.
22. Yuanzhi Tang, Helen F. Chappell, Martin T. Dove, Richard J. Reeder, Young J. Lee, "Zinc incorporation into hydroxylapatite", Biomaterials, Vol.30, pp.2864–2872, 2009.
23. Vojislav Stanić, Suzana Dimitrijević, Jelena Antić-Stanković, Miodrag Mitrić, Bojan Jokić, Ilija B. Plećaš, Slavica Raićević, "Synthesis, characterization and antimicrobial activity of copper and zinc-doped hydroxyapatite nanopowders", Appl. Sur. Sci., Vol.256, pp.6083–6089, 2010.
24. Danielle Laurencin, Neyvis Almora-Barrios, Nora H. de Leeuw, Christel Gervais, Christian Bonhomme, Francesco Mauri, Wojciech Chrzanowski, Jonathan C. Knowles, Robert J. Newport, Alan Wong, Zhehong Gan, Mark E. Smith, "Magnesium incorporation into hydroxyapatite", Biomaterials, Vol.32, pp.1826-1837, 2011.
25. A. Gozalian, A. Behnamghader, M. Daliri, A. Moshkforoush, "Synthesis and thermal behavior of Mg-doped calcium phosphate nanopowders via the sol gel method", Scientia Iranica F, Vol.18, No.6, pp.1614–1622, 2011.
26. T. Kokubo, H. Kushitani, S. Sakka, T. Kitsugi and T. Yamamuro, "Solutions able to reproduce in vivo surface-structure changes in bioactive glass-ceramic A-W", J. Biomed. Mater. Res., Vol.24, pp.721-734, 1990.